Experimental investigation on wettability alteration of Glauconitic sandstone during CO_2 Storage.

Wael F. Al-Masri[1*], *Samira* Mohammadkhani[1], *Bettina* Jenei[2], *Behzad* Rostami[1]

[1] Geological Survey of Denmark and Greenland (GEUS), Department of Geo-energy and Storage, 1350 Copenhagen K, Denmark
[2] Clausthal University of Technology, Institute of Subsurface Energy Systems, 38678 Clausthal-Zellerfeld, Germany

Abstract. This study explores wettability alteration resulting from supercritical CO_2 ($scCO_2$) injection into Glauconitic sandstone in the depleted Nini West oil reservoir (Danish North Sea), evaluating its potential for CO_2 storage. Injected $scCO_2$ dissolves in brine and diffuses into residual oil, displacing adsorbed hydrocarbons and shifting the rock surface toward a more water-wet state. This enhances residual oil displacement and increases CO_2 storage efficiency. Wettability was assessed using spontaneous imbibition experiments on core samples from the oil and water legs. Among them, two samples from the oil leg were flooded under reservoir conditions using brine, followed by $scCO_2$. Results show that $scCO_2$ exposure significantly increased water-wetness, with water saturation reaching 55% in $scCO_2$-flooded oil-leg cores. In contrast, cores cleaned using Soxhlet extraction or flow-through solvent methods remained less water-wet, with average water saturations below 30%. These findings indicate that $scCO_2$ acts as an effective agent for altering wettability in previously oil-wet, watered-out porous media systems, altering CO_2 trapping potential. This work supports the use of depleted oil reservoirs for geological CO_2 storage, emphasising $scCO_2$'s role in improving storage performance through wettability modification.

1 Introduction

Storing carbon dioxide (CO_2) underground on a large scale is seen as a promising way to reduce greenhouse gas emissions to the atmosphere [1]. There are mainly three geological options for CO_2 storage: depleted oil and gas reservoirs, deep saline aquifers, and coalbeds that cannot be mined [2].

When CO_2 is injected into deep saline aquifers, a caprock layer usually acts as a seal, stopping the upward movement of CO_2. This mechanism is known as structural or primary trapping, accounting for most trapped CO_2 [3]. Another key mechanism, called capillary or residual trapping, happens during the process of re-imbibition. As the CO_2 plume migrates, water re-enters the pores behind it, leaving behind disconnected CO_2 clusters [4]. To improve CO_2 storage efficiency in saline aquifers, it's important to understand the behaviour of spontaneous imbibition in porous rocks [5].

Spontaneous imbibition refers to the natural movement of a wetting fluid, like water, into pore spaces filled with a non-wetting fluid, such as CO_2, driven by capillary forces [6]. This process is important in many fields, including CO_2 storage, soil clean-up, and oil recovery from fractured rocks [7]. Many researchers have studied spontaneous imbibition using both laboratory tests and computer simulations [8, 9]. Earlier studies have mostly focused on predicting how fast imbibition happens [10, 11], how much non-wetting fluid gets trapped [12], and how capillary pressure and relative permeability behave on a larger scale [13]. However, two key aspects—how quickly the fluid is recovered and how the trapped gas phase develops—still need more attention. Studies have explored how the residual gas saturation forms during spontaneous imbibition under normal conditions [14, 15, 16].

A wide range of experiments and theoretical work has shown that the speed and amount of spontaneous imbibition are mainly influenced by rock and fluid properties such as porosity, permeability, viscosity, interfacial tension, and wettability [17, 18, 19]. However, other research suggests that the final recovery of the non-wetting phase is also heavily affected by how the rock and fluids interact [21, 22, 23]. Therefore, factors like the mineralogical content of the rock and the chemical composition of both the injected and original fluids should be considered when evaluating how effective spontaneous imbibition might be [24, 25].

Among all these factors, wettability is one of the most critical ones. It directly affects structural and capillary trapping during CO_2 storage in deep saline aquifers [26, 27, 28, 29]. It also indirectly impacts CO_2 dissolution and mineral trapping by influencing the interaction at the gas-

* Corresponding author: wfa@geus.dk

liquid-rock interfaces [30, 31]. Over time, various chemical reactions—like acid-base interactions and mineral dissolution—can change the wettability of the rock, affecting how much CO_2 can be stored and how well it remains trapped underground [32, 33, 34].

Changes in wettability also affect capillary pressure, which influences how well the fluid spreads through the pores. These changes can either enhance or harm the efficiency and capacity of CO_2 storage. For example, certain changes inside the reservoir can increase residual trapping [49, 52]. On the other hand, if wettability shifts from strongly to weakly water-wet in quartz, it may reduce both structural and residual trapping [47]. Changes in the caprock's wettability can also reduce its sealing ability [50, 51]. These effects highlight the need to understand how supercritical CO_2 ($scCO_2$) exposure changes the wettability of sandstone.

The impact of wettability changes during CO_2 flooding has been widely studied using core-scale experiments [35, 36, 37, 38]. These studies have confirmed that injecting CO_2 can indeed alter the wettability of rocks. In many cases, a drop in interfacial tension has also contributed to this change [39].

Researchers have explored many factors that affect how wettability changes when rocks are exposed to CO_2. These include the physical features of the rock, fluid chemistry, and conditions like pressure and temperature. Experiments show that formation brine salinity, surface roughness, rock mineralogical composition, CO_2 density and concentration, and CO_2 exposure time all influence wettability in subsurface formations [40, 41, 47, 53].

This study focuses on spontaneous imbibition tests that have been utilised to explore how different original properties of rock samples affect the trapping of CO_2. The primary objective is to estimate the wettability difference between core samples collected from the oil-leg (Nina4) and the water-leg (Nina4a) of the reservoir qualitatively, understand how different cleaning methods affect wettability, and observe changes in wettability due to $scCO_2$ injection. The flooding experiment was conducted at a fluid pressure of 200 bar and a temperature of 60 °C. For each spontaneous imbibition, a quantitative analysis was performed by comparing the volume of displaced water recorded during the immersion of the core sample in brine.

2 Materials and Methods

2.1 Materials

Core plug samples used in this study originate from glauconite-rich sandstones of Palaeocene–Eocene age, deposited in a deep marine environment and hosted within mudstone intervals of the Nini West Field, located in the Danish sector of the North Sea. This field, a depleted oil reservoir, is currently being evaluated for its potential suitability for geological CO_2 storage. The reservoir sandstones are characterised by their fine grain size, good sorting, and a notable mineralogical composition consisting predominantly of quartz with approximately 20–30% glauconite. These textural and compositional features contribute to the high porosity and permeability of the formation, making it an attractive candidate for subsurface CO_2 injection.

Previous investigations have revealed that the reservoir rock displays a mixed-wet to strongly oil-wet wettability profile. This condition is primarily attributed to the persistent presence of non-movable hydrocarbon components—specifically solid bitumen and asphaltenes—that are tenaciously bound to glauconite grains and glauconitised mica surfaces. A suite of organic geochemical and petrographic analyses was conducted on core plugs that were preserved, solvent-cleaned, restored to original wettability conditions, and subjected to supercritical CO_2 ($scCO_2$) flooding. These analyses demonstrated that, even after rigorous cleaning and $scCO_2$ exposure under simulated reservoir conditions, the heavy hydrocarbon residues remained adhered to mineral surfaces. This observation underscores the robustness of the rock's wettability characteristics. Such wettability resilience may contribute positively to formation integrity by limiting mineral dissolution and reducing the risk of fines migration, which are both critical factors for safe and effective long-term CO_2 storage [54].

A total of six cylindrical core plugs (1.5-inch diameter) were selected for the study. Two plugs, designated WL1 and WL2, were obtained from the water leg of well Nini-4a, representing brine-saturated zones. Four additional plugs—OL1, OL2, CF1, and CF2—were extracted from the oil leg of well Nini-4, corresponding to zones with a history of hydrocarbon saturation.

Table 1 Petrophysical properties of the core plugs used in this study. Data include plug depth, porosity (ϕ), air permeability (kair), grain density (ρ_grain), bulk volume (Vb), and pore volume (Vp).

Plug ID	Depth, MD [m]	Well	ϕ [%]	k_{air} [mD]	ρ_{grain} [g/ml]	V_b [ml]	Vp [ml]
WL1	1933.54	Nini-4A	39.00	1500	2.72	52.37	20.43
WL2	1938.04	Nini-4A	39.20	1130	2.74	49.64	19.46
OL1	1774.03	Nini-4	35.80	1280	2.70	55.34	19.81
OL2	1775.97	Nini-4	34.84	1023	2.71	63.94	22.27
CF1	1776.95	Nini-4	36.00	1248	2.72	70.01	25.21
CF2	1776.97	Nini-4	36.00	1270	2.72	70.24	25.30

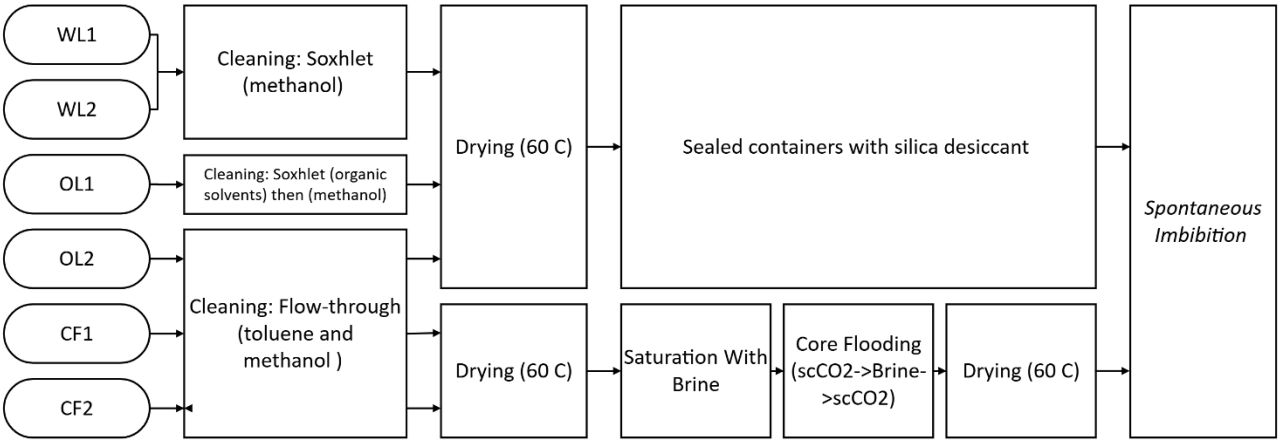

Fig. 1 Experimental workflow for each core plug, from cleaning and drying to $scCO_2$ flooding (CF1 and CF2 only) and final spontaneous imbibition testing.

The sample selection strategy was designed to encompass the two wettability maxima as a reference. All core plugs were taken perpendicular to bedding to minimise anisotropy effects and avoid natural fractures or visible heterogeneities. The petrophysical properties of the core samples are summarised in Table 1.

The synthetic formation brine used in the study was formulated to match the composition and salinity of the reservoir's formation water, with a total dissolved solids (TDS) content of 87,000 ppm. The brine composition was dominated by Na^+ and Cl^- ions, with contributions from Ca^{2+}, Mg^{2+}, K^+, Ba^{2+}, Sr^{2+}, HCO_3^- and SO_4^{2-}, consistent with the geochemical data reported for the Nini Field aquifer system. The CO_2 used in this study had a certified purity grade of 4.0 (99.99%) and was used for the core flooding experiments conducted under controlled temperature and pressure conditions simulating those of the reservoir

2.2 Methods

This section describes the experimental procedures used to investigate wettability alteration in glauconitic Greensand core plugs subjected to supercritical CO_2 flooding. The workflow included a detailed description of the core cleaning methods, core flooding, and spontaneous imbibition tests to evaluate wettability states. Core plugs were selected from both the water and oil legs of the Nini West Field, with cleaning protocols tailored to their initial saturation history. Figure 1 provides an overview of the experimental path followed by each individual core plug, from initial treatment through to the spontaneous imbibition test.

2.2.1 Cleaning process

Sample cleaning procedures were selected based on the expected hydrocarbon content derived from core origin. The water-leg samples (WL1 and WL2), which contained no hydrocarbons, were cleaned using Soxhlet extraction with methanol only. This method was adequate for removing residual formation water and salts. Cleaning was conducted externally by Robertson Research International (RRI), in accordance with API-recommended procedures.

Sample OL1, obtained from the oil leg, underwent a more rigorous Soxhlet cleaning protocol. The plug was initially exposed to an azeotropic solvent mixture of chloroform, methanol, and methylamine to dissolve asphaltenes and bitumen, followed by toluene and finally methanol to eliminate any remaining organics and salts. The cleaning process extended over several weeks, and the effluent was visually inspected under UV light to confirm the complete removal of hydrocarbons.

Samples OL2, CF1, and CF2 were cleaned using an in-house flow-through method at GEUS. These samples were alternately flushed with toluene and methanol at ambient laboratory temperature under controlled backpressure. The cleaning continued until the effluent became colourless and tested negative for chloride ions when mixed with silver nitrate solution, ensuring both hydrocarbons and salts were fully removed. The net overburden pressure during flushing was kept below 5 bar, and flow rates were maintained at approximately 5 mL/h to prevent structural alteration of the pore system. Drying was performed at 60 °C in a ventilated oven, and samples were considered fully dry once their mass stabilised over two consecutive 24-hour intervals. To minimise any moisture uptake or contamination from atmospheric humidity, all core plugs were immediately transferred to sealed containers with silica desiccant before any further processing.

2.2.2 Core Flooding Procedure

The core flooding experiment was conducted to evaluate the wettability alteration induced by $scCO_2$ exposure. This two-phase experiment was performed on samples CF1 and CF2, which were cleaned and dried as previously described, before being saturated with synthetic Nini formation brine to fill the pore space (Sw = 1.0) completely. The plugs were assembled in a horizontal configuration within a hydrostatic core holder, positioned between two fine steel mesh filters (40 µm grid) to prevent the transport of loose fines during injection. See Figure 2.

.

Fig. 2 Core assembly for sample CF1 to the left (inlet), and sample CF2 to the right (outlet). Adjacent to the core samples are the two filters with a 40 µm mesh size.

The core holder was mounted in the GEUS flooding rig, and all operations were conducted under simulated reservoir conditions: a temperature of 60 °C, a pore pressure of 200 bar, and a net overburden of 25 bar. The system was filled with synthetic Nini formation brine. Initial brine permeability was determined by injecting 4.2 pore volumes (PVs) at 100 mL/h, resulting in an absolute liquid permeability of 858 mD.

The first CO_2 flooding sequence was initiated by injecting 64.2 PVs of $scCO_2$ at a rate of 800 mL/h. This was succeeded by a higher-rate injection of 106.1 PVs at 1740 mL/h. Water production was monitored in real time using a two-phase acoustic separator (NISEP). After CO_2 flooding, a brine flood was conducted in the reverse flow direction. A total of 13.2 PVs of synthetic brine were injected at 100 mL/h. This was followed by a second CO_2 injection, replicating the first $scCO_2$ injection: 64.4 PVs at 800 mL/h, followed by 130.4 PVs at 1740 mL/h.

After completing the flooding sequence, the system was slowly depressurised and cooled while utilising backpressure regulation to prevent CO_2 expansion artefacts. The core holder was then disassembled, and both plugs were dried at 60 °C to assess post-flood residual water saturation. Final water saturation values were estimated gravimetrically (2.65% for CF1 and 14.56% for CF2). These samples were then prepared for spontaneous imbibition tests, as described below, to evaluate wettability alteration. For full results of the core flooding experiment, the reader is referred to [55].

2.2.3 Spontaneous Imbibition

Spontaneous imbibition tests were performed on all six core plugs (WL1, WL2, OL1, OL2, CF1, CF2) to evaluate their wettability states under various conditions. This method offers both qualitative and quantitative indicators of the rock's capillary-driven affinity for water.

Dried samples were weighed to obtain the baseline dry mass. Each plug was then suspended vertically from a metal L-bracket mounted on a METTLER PM 480 precision balance (±0.001 g), ensuring that the sample was freely suspended and isolated from vibrations. A glass beaker filled with synthetic brine was mounted on a laboratory jack and raised until the brine submerged the core, and the water level reached a predefined reference height. The position of the water surface was regularly checked and adjusted to maintain a constant immersion depth during the experiment. See Figure 3.

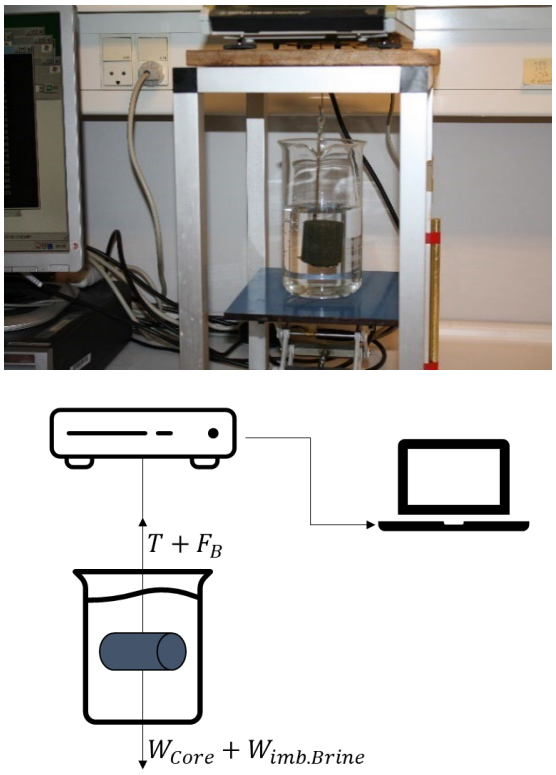

Fig. 3 *Spontaneous imbibition setup. Top: laboratory configuration. Bottom: illustrates the working principle: the total measured force indicates brine uptake by the core, recorded digitally via a connected balance.*

When the core sample is submerged in brine, it is subjected to the following forces: its own weight, W_{core}, and the weight of the imbibed brine, $W_{imb\cdot Brine}$, both acting downward and the tension in the cored, scale reading T, and the buoyancy force, F_B, both acting upward and net forces acting on it at any moment are equal to zero since the core is stagnant in space according to Newton's second law and can be expressed mathematically as follows:

$$T = W_{Core} + W_{imb\cdot Brine} - F_b \quad (1)$$

According to the Archimedes principle, the buoyancy force is equal to the weight of the fluid that the body displaces. Thus:

$$F_b = \rho_{brine}\, g\, V_{Core} \quad (2)$$

here, ρ_{Brine} is the brine density, g is the gravitational acceleration, and V_{core} is the volume of the core sample. Since the weight and the volume of the core sample do not change with time, any change in the scale reading is due to an increase in the amount of imbibed brine, and it reads:

$$\frac{dT}{dt} = \frac{dW_{imb\cdot Brine}}{dt} \quad (3)$$

Weight gain from imbibed brine was recorded automatically at 10-second intervals for the first 24 hours, after which the interval was extended to 15 seconds. The test was deemed complete when no weight change was observed over a three-hour period. Following this, suspended and submerged weights were noted to determine the core's total volume and brine saturation using Archimedes' principle.

The cumulative brine uptake over time was utilised to calculate the final water saturation and interpret the sample's wettability. Water-leg samples served as a water-wet baseline, whereas oil-leg samples (cleaned or flooded) provided insights into the degree of wettability alteration. The $scCO_2$-flooded samples (CF1 and CF2) were of particular interest, as the wettability changes induced by CO_2-brine–mineral interactions can significantly impact capillary trapping and storage efficiency in CO_2 storage operations.

3 Results and Discussion

3.1 Water-leg samples (WL1 and WL2)

Spontaneous imbibition tests on samples WL1 and WL2, retrieved from the water leg of the reservoir, demonstrated rapid brine uptake upon contact. This was visually confirmed by continuous gas bubbling from the top of the cores (Figure 4) and a steep increase in mass readings from the balance. Additionally, significant grain loss occurred during early contact, with approximately 0.5 g of dislodged material collected, dried, and quantified (Figure 4). Corrections for this mass loss were implemented in subsequent saturation calculations.

Figure 5 presents the quantitative results. Both samples exhibited nearly identical imbibition behaviour—rapid initial uptake followed by early equilibrium, reaching final brine saturations of 69.5% (WL1) and 70.6% (WL2). The consistency between replicates highlights the reproducibility of the method. These results indicate a strongly water-wet system, as anticipated for glauconitic sandstone from the brine-saturated zone, which is primarily composed of quartz and glauconite with minimal organic content.

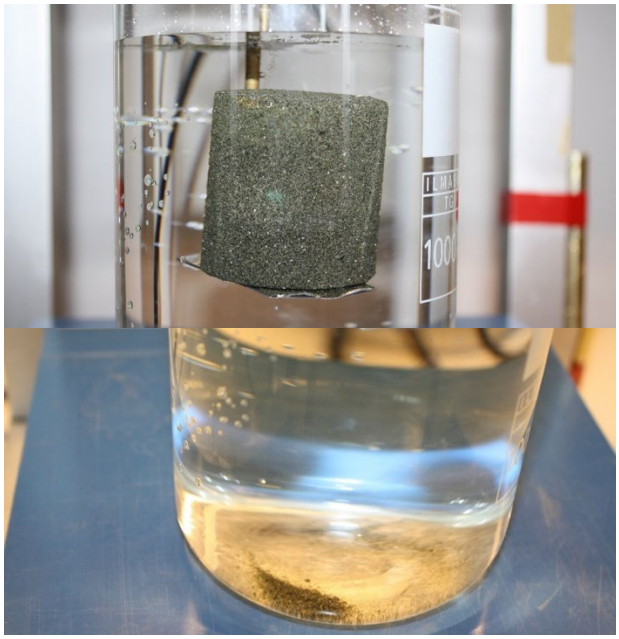

Fig. 4 *A water-leg sample after immersion in Nini formation brine (top), and the fines remain in the beaker glass after the imbibition test is completed (bottom).*

3.2 Oil-leg Samples (OL1 and OL2)

In contrast to the water-leg cores, the oil-leg samples OL1 and OL2 exhibited slower imbibition rates and a weaker affinity for water. Visual observations revealed intermittent, disconnected gas bubbles escaping from the core over an extended period. Almost no grain loss was noted, suggesting stronger grain cohesion, likely due to the presence of residual bitumen or asphaltenes acting as an adhesive layer on mineral surfaces.

Quantitative data (Figure 6) show significantly lower final brine saturations: 42.15% for OL1 and 32.57% for OL2. OL1, cleaned via hot Soxhlet extraction, reached equilibrium within 25 hours, while OL2, cleaned by flow-through solvent flushing, required over 40 hours to stabilise. The results suggest that cleaning efficiency directly impacts wettability alteration. Soxhlet cleaning appeared more effective in removing organic residues than the flow-through method, consistent with the higher brine saturation in OL1. Nevertheless, both samples remained in a mixed-wet to weakly oil-wet state.

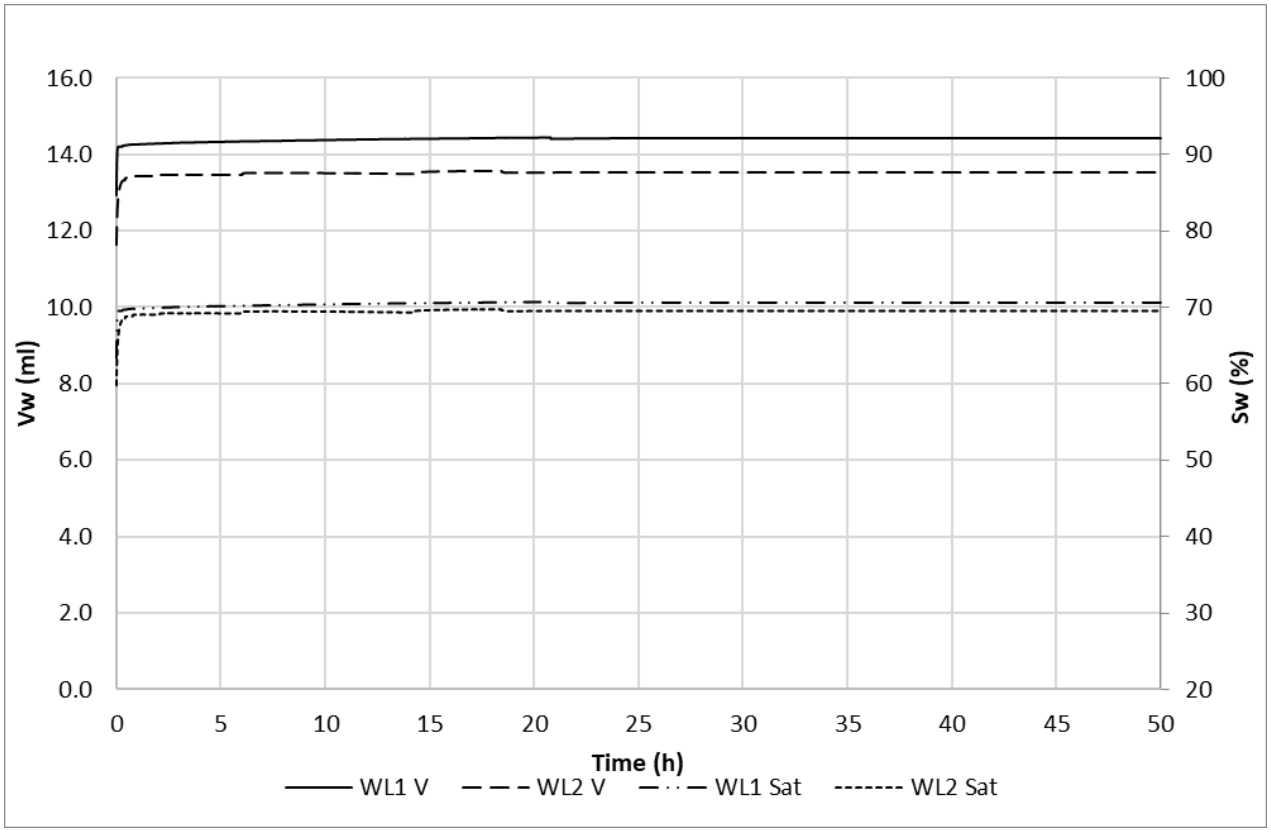

Fig. 5 Brine uptake (Vw) and water saturation (Sw) over time for water-leg samples WL1 and WL2. Both cores show rapid imbibition and reach stable, high saturations (~70%), indicating strongly water-wet conditions

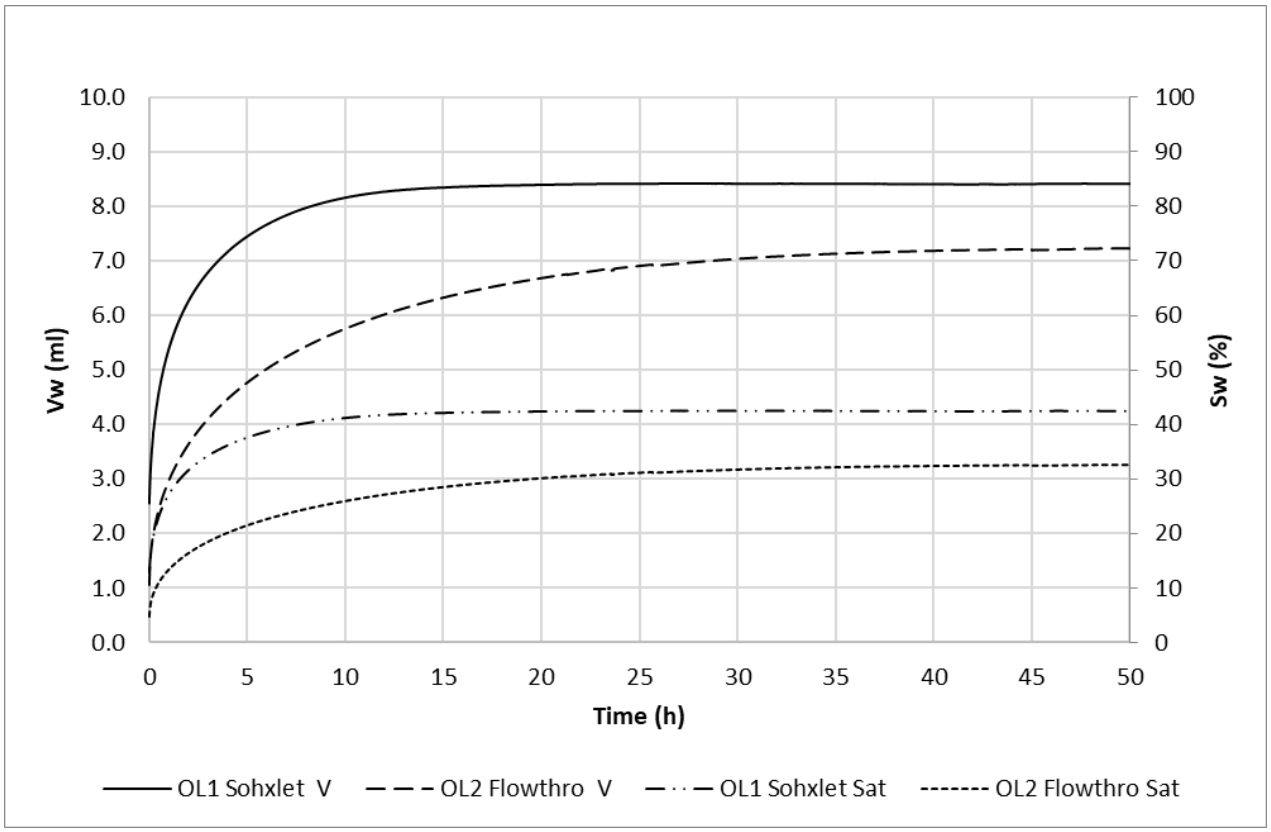

Fig. 6 *Brine uptake (Vw) and water saturation (Sw) versus time for oil-leg samples OL1 (Soxhlet cleaned) and OL2 (flow-through cleaned). Both show slower, lower imbibition compared to water-leg samples, with OL1 reaching 42.2% and OL2 only 32.6%, indicating mixed-to-weakly oil-wet behaviour.*

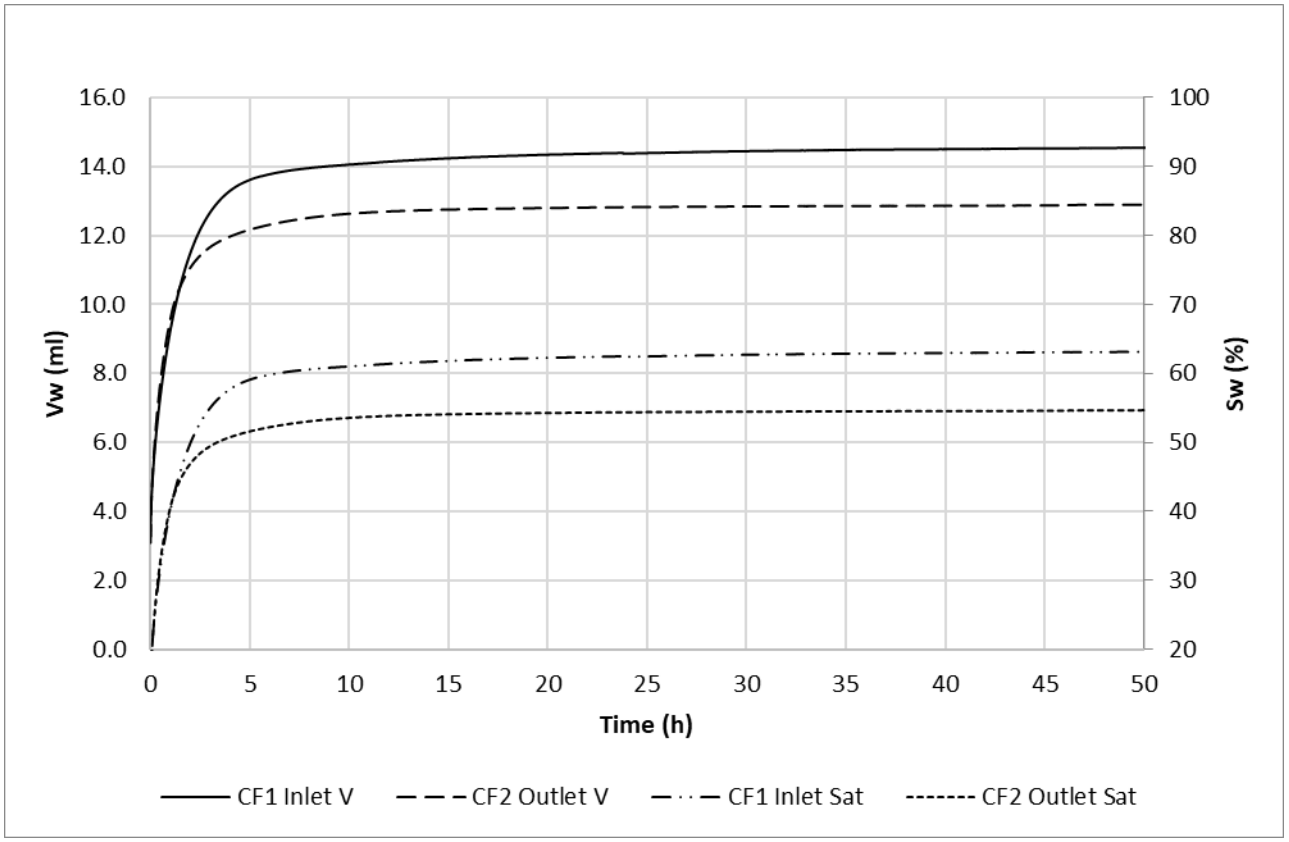

***Fig. 7** Brine uptake (Vw) and water saturation (Sw) over time for CO_2-flooded samples CF1 (inlet) and CF2 (outlet). Both cores show moderate imbibition, with final saturations of 63.2% (CF1) and 55.1% (CF2), indicating a significant shift toward more water-wet conditions post-scCO_2 exposure.*

3.3 CO2-flooded samples (CF1 and CF2)

Samples CF1 and CF2, which underwent core flooding with supercritical CO_2 under reservoir conditions, exhibited intermediate imbibition characteristics between the water-leg and cleaned oil-leg samples. Like the latter, gas bubble emission was intermittent, and grain loss was negligible, suggesting the structural integrity of the pore network was maintained post-flooding.

As shown in Figure 7, both samples exhibited nearly identical imbibition behaviour in the first 1.5 hours. After this point, the brine uptake rate in CF2 (the outlet plug) declined more rapidly than CF1 (the inlet plug). Final brine saturations were 55.08% (CF2) and 63.16% (CF1). This difference may be attributed to partial wettability alteration: in CF2, approximately 14.65% of the pore volume remained brine-saturated during CO_2 injection and thus may not have experienced full wettability shift. In contrast, only 2.65% of CF1's pore space retained brine post-flooding, suggesting a broader extent of CO_2 contact and alteration.

3.4 Discussion

The results clearly indicate that exposure to supercritical CO_2 induces a shift in wettability towards a more water-wet state in glauconitic sandstone. This effect was compared against oil-leg samples subjected to solvent cleaning. Notably, scCO_2-flooded samples (CF1, CF2) demonstrated significantly higher final brine saturations than their cleaned but unflooded counterparts (OL1, OL2). Despite OL1 undergoing an aggressive Soxhlet cleaning procedure, its final saturation remained lower than that of the CO_2-flooded samples.

Figure 8 summarises the comparative performance of all six samples. The CO_2-flooded plugs exhibited greater wettability alteration than OL2 (cleaned by the same method used for CF1 and CF2 prior to flooding) and even surpassed OL1, which had been cleaned with stronger organic solvents. This suggests that scCO_2 is capable of displacing adsorbed hydrocarbons from mineral surfaces more effectively, potentially due to its low viscosity, small molecular size, and ability to access finer pore structures. Furthermore, the drying phase between brine and CO_2 injections may have contributed to salt layer precipitation and altered capillary interactions, further enhancing wettability change.

Although the brine uptake rates in CO_2-flooded samples were slower than those in the water-leg samples, the final saturation in CF1 approached the values of WL1 and WL2, differing by only 6.36% and 7.44%, respectively. This suggests that the wettability in CF1 was significantly altered towards water-wet conditions, comparable to naturally water-wet rock, facilitating the removal of oil from smaller pores, which can explain the substantial shift in wettability.

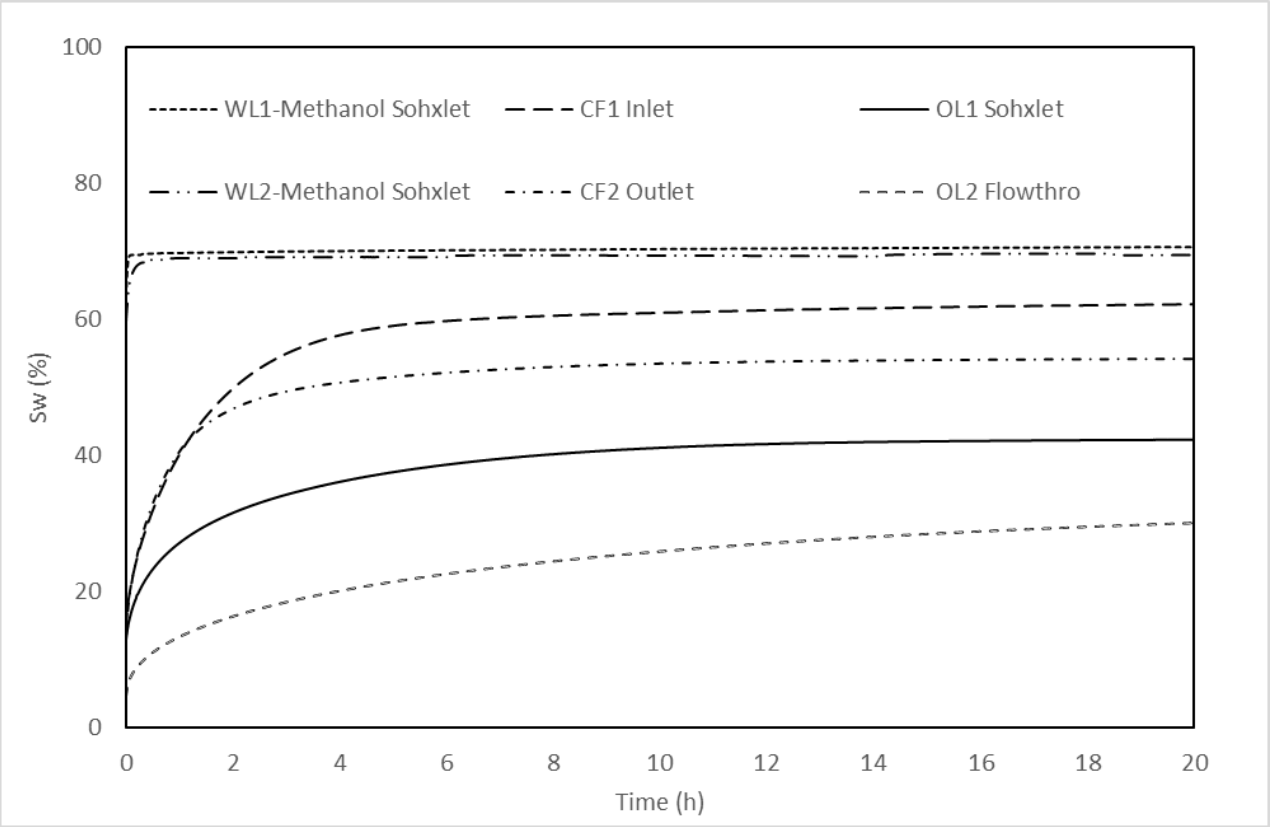

Fig. 8 *Comparison of water saturation (Sw) over time for all core plugs. CO_2-flooded samples (CF1, CF2) show significantly higher final saturations than oil-leg samples cleaned with Soxhlet (OL1) or flow-through (OL2) methods, and approach the values observed in water-leg samples (WL1, WL2), demonstrating effective wettability alteration by $scCO_2$.*

4 Conclusions

This study examined the impact of supercritical CO_2 exposure on the wettability of glauconitic sandstone from the Nini West Field. Six core plugs were tested using spontaneous imbibition experiments, including two CO_2-flooded samples (CF1 and CF2), two cleaned oil-leg samples (OL1 and OL2), and two water-leg reference samples (WL1 and WL2). Core flooding of CF1 and CF2 was conducted under representative reservoir conditions (200 bar, 60 °C), followed by spontaneous imbibition under ambient conditions.

The results demonstrate that $scCO_2$ exposure leads to substantial alterations in wettability, shifting the rock surface towards a more water-wet state. The final brine saturations of CF1 and CF2 (63.2% and 55.1%, respectively) significantly exceeded those of solvent-cleaned oil-leg samples (32.6% and 42.2%), approaching values measured in water-leg samples (~70%). This indicates that $scCO_2$ is a more effective agent for modifying surface wettability in this mineralogical system than traditional organic solvents.

These findings suggest that $scCO_2$ plays a dual role in geological storage operations—not only as a storable fluid but also as an in-situ wettability modifier that changes capillary trapping. The observed trends support the viability of deploying CO_2 injection in previously oil-wet reservoirs, where improved wettability alteration can enhance storage capacity, reduce residual oil saturation, and mitigate injectivity risks associated with fines migration and mineral instability.

This research was conducted as part of Project Greensand Phase 2, an initiative focused on the safe and permanent storage of CO_2 within the depleted Nini West oil reservoir located in the Siri Canyon of the Danish North Sea. Project Greensand Phase 2 is a collaborative effort, comprising a consortium of 23 Danish and international partners from both industry and academia, working collectively to advance carbon capture and storage (CCS) technologies. The project is generously supported by the Danish Energy Technology Development and Demonstration Program (EUDP) under grant agreement #64021-9005, whose funding has been instrumental in enabling the scientific investigations and technological innovations presented in this study.

References

1. International Energy Agency (2004). *Prospects for CO_2 Capture and Storage*. Paris: OECD/IEA.
2. M. Bui, C.S. Adjiman, A. Bardow, et al. (2018). *Carbon capture and storage (CCS): the way forward.* Energy & Environmental Science, **11**(5), 1062–1176.
3. P. Egermann, J.-M. Lombard, P. Bretonnier (2006). *A fast and accurate method to measure threshold capillary pressures under representative conditions.*

SCA A46, presented at the SCA International Symposium, Trondheim, September 18–22.
4. R. Juanes, E.J. Spiteri, F.M. Orr, M.J. Blunt (2006). *Impact of relative permeability hysteresis on geological CO_2 storage*. Water Resources Research, **42**(12), 1–13.
5. M. Mahdaviara, M. Sharifi, S. Bakhshian, N. Shokri (2022). *Prediction of spontaneous imbibition in porous media using deep and ensemble learning techniques*. Fuel, **329**, 125349.
6. N. Morrow, G. Mason (2001). *Recovery of oil by spontaneous imbibition*. Current Opinion in Colloid & Interface Science, **6**(4), 321–337.
7. Q. Meng, H. Liu, J. Wang (2017). *A critical review on fundamental mechanisms of spontaneous imbibition and the impact of boundary condition, fluid viscosity and wettability*. Advances in Geo-Energy Research, **1**(1), 1–17.
8. B.J. Bourbiaux, F.J. Kalaydjian (1990). *Experimental study of cocurrent and countercurrent flows in natural porous media*. SPE Reservoir Engineering, **5**(3), 361–368.
9. H.A. Nooruddin, M.J. Blunt (2016). *Analytical and numerical investigations of spontaneous imbibition in porous media*. Water Resources Research, **52**(9), 7284–7310.
10. S. Akin, J.M. Schembre, S.K. Bhat, A.R. Kovscek (2000). *Spontaneous imbibition characteristics of diatomite*. Journal of Petroleum Science and Engineering, **25**(3–4), 149–165.
11. C. Hall, V. Pugsley (2020). *Spontaneous capillary imbibition of water and nonaqueous liquids into dry quarry limestones*. Transport in Porous Media, **135**(3), 619–631.
12. Q. Meng, H. Liu, J. Wang (2015). *Entrapment of the non-wetting phase during co-current spontaneous imbibition*. Energy & Fuels, **29**(2), 686–694.
13. N. Alyafei, M.J. Blunt (2018). *Estimation of relative permeability and capillary pressure from mass imbibition experiments*. Advances in Water Resources, **115**, 88–94.
14. G. Mason, N.R. Morrow (2013). *Developments in spontaneous imbibition and possibilities for future work*. Journal of Petroleum Science and Engineering, **110**, 268–293.
15. K. Li, R.N. Horne (2001). *Characterization of spontaneous water imbibition into gas-saturated rocks*. SPE Journal, **6**(4), 375–384.
16. P. Egermann, J.-M. Lombard, P. Bretonnier (2004). *Experimental and numerical study of water–gas imbibition phenomena in vuggy carbonates*. Paper SPE 89421, presented at the SPE/DOE 14th Symposium on Improved Oil Recovery, Tulsa, April 17–21.
17. J. Cai, E. Perfect, C.-L. Cheng, X. Hu (2014). *Generalised modelling of spontaneous imbibition based on Hagen-Poiseuille flow in tortuous capillaries with variably shaped apertures*. Langmuir, **30**(18), 5142–5151.
18. M. Seyyedi, M. Sohrabi (2016). *Enhancing water imbibition rate and oil recovery by carbonated water in carbonate and sandstone rocks*. Energy & Fuels, **30**(1), 285–293.
19. H.O. Yildiz, M. Gokmen, Y. Cesur (2006). *Effect of shape factor, characteristic length, and boundary conditions on spontaneous imbibition*. Journal of Petroleum Science and Engineering, **53**(3–4), 158–170.
20. L. Gao, Z. Yang, Y. Shi (2018). *Experimental study on spontaneous imbibition characteristics of tight rocks*. Advances in Geo-Energy Research, **2**(3), 292–304.
21. S. Akin, J.M. Schembre, S.K. Bhat, A.R. Kovscek (2000). *Spontaneous imbibition characteristics of diatomite*. Journal of Petroleum Science and Engineering, **25**(3–4), 149–165.
22. C.U. Hatiboglu, T. Babadagli (2010). *Experimental and visual analysis of co- and countercurrent spontaneous imbibition for different viscosity ratios, interfacial tensions, and wettabilities*. Journal of Petroleum Science and Engineering, **70**(3–4), 214–228.
23. N. Alyafei, A. Al-Menhali, M.J. Blunt (2016). *Experimental and analytical investigation of spontaneous imbibition in water-wet carbonates*. Transport in Porous Media, **115**(1), 189–207.
24. H. Roshan, S. Ehsani, C.E. Marjo, M.S. Andersen, R.I. Acworth (2015). *Mechanisms of water adsorption into partially saturated fractured shales: an experimental study*. Fuel, **159**, 628–637.
25. M. Mehana, M. Al Salman, M. Fahes (2018). *Impact of salinity and mineralogy on slick water spontaneous imbibition and formation strength in shale*. Energy & Fuels, **32**(5), 5725–5735.
26. R. Hu, J. Wan, Y. Kim, T.K. Tokunaga (2017). *Wettability impact on supercritical CO_2 capillary trapping: pore-scale visualization and quantification*. Water Resources Research, **53**(7), 6377–6394.
27. A. Baban, A. Keshavarz, R. Amin, S. Iglauer (2022). *Impact of wettability alteration on CO_2 residual trapping in oil-wet sandstone at reservoir conditions using nuclear magnetic resonance*. Energy & Fuels, **36**(12), 13722–13731.
28. L.M. Valle, R. Rodríguez, C. Grima, C. Martínez (2018). *Effects of supercritical CO_2 injection on sandstone wettability and capillary trapping*. International Journal of Greenhouse Gas Control, **78**, 341–348.
29. S. Iglauer, A.Z. Al-Yaseri, R. Rezaee, M. Lebedev (2015). *CO_2 wettability of caprocks: implications for structural storage capacity and containment security*. Geophysical Research Letters, **42**(23), 9279–9284.
30. E.A. Al-Khdheeawi, S. Vialle, A. Barifcani, M. Sarmadivaleh, S. Iglauer (2017). *Influence of CO_2-wettability on CO_2 migration and trapping capacity in deep saline aquifers*. Greenhouse Gases: Science and Technology, **7**(2), 328–338.
31. C. Qin, Y. Jiang, J. Zhou, S. Zuo, S. Chen, Z. Liu, H. Yin, Y. Li (2022). *Influence of supercritical CO_2 exposure on water wettability of shale: implications for CO_2 sequestration and shale gas recovery*. Energy, **242**, 122551.

32. J. Rohmer, A. Pluymakers, F. Renard (2016). *Mechano-chemical interactions in sedimentary rocks in the context of CO_2 storage: weak acid, weak effects?* Earth-Science Reviews, **157**, 86–110.
33. Q. Liu, M.M. Maroto-Valer (2011). *Parameters affecting mineral trapping of CO_2 sequestration in brines*. Greenhouse Gases: Science and Technology, **1**(3), 211–222.
34. A. Fatah, Z. Bennour, H.B. Mahmud, R. Gholami, M. Hossain (2021). *Surface wettability alteration of shales exposed to CO_2: implication for long-term integrity of geological storage sites*. International Journal of Greenhouse Gas Control, **110**, 103426.
35. G.F. Potter (1987). *The effects of CO_2 flooding on wettability of West Texas dolomitic formations*. Paper SPE 16716 presented at the Annual Technical Conference and Exhibition, Dallas, September 27–30.
36. M. Vives, Y. Chang, K. Mohanty (1999). *Effect of wettability on adverse-mobility immiscible floods*. SPE Journal, **4**(3), 260–267.
37. S.M. Al-Mutairi, S.A. Abu-Khamsin, T.M. Okasha, M.E. Hossain (2014). *An experimental investigation of wettability alteration during CO_2 immiscible flooding*. Journal of Petroleum Science and Engineering, **120**, 73–77.
38. Y. Chen, A. Sari, Q. Xie, A. Saeedi (2019). *Insights into the wettability alteration of CO_2-assisted EOR in carbonate reservoirs*. Journal of Molecular Liquids, **279**, 420–426.
39. A. Shariat, R. Moore, S. Mehta, K. Van Fraassen, K. Newsham, J. Rushing (2012). *Laboratory measurements of CO_2–H_2O interfacial tension at HP/HT conditions: implications for CO_2 sequestration in deep aquifers*. Paper CMTC 150010 presented at the Carbon Management Technology Conference, Orlando, February 7–9.
40. M. Arif, S.A. Abu-Khamsin, S. Iglauer (2019). *Wettability of rock/CO_2/brine and rock/oil/CO_2-enriched-brine systems: critical parametric analysis and future outlook*. Advances in Colloid and Interface Science, **268**, 91–113.
41. A.M. Kassa, S.E. Gasda, K. Kumar, F.A. Radu (2020). *Impact of time-dependent wettability alteration on the dynamics of capillary pressure*. Advances in Water Resources, **142**, 103631.
42. P. Lv, Y. Liu, Z. Wang, S. Liu, L. Jiang, J. Chen, Y. Song (2017). *Langmuir*, **33**, 3358.
43. P.I. Sagbana, K. Sarkodie, W.A. Nkrumah (2022). *Petroleum*, **9**, 317.
44. K. Chaudhary, E.J. Guiltinan, M.B. Cardenas, J.A. Maisano, R.A. Ketcham, P.C. Bennett (2015). *Geochemistry, Geophysics, Geosystems*, **16**, 2858.
45. A. Daryasafar, A. Keykhosravi, K. Shahbazi (2019). *Journal of Cleaner Production*, **239**, 118101.
46. P. Chiquet, D. Broseta, S. Thibeau (2007). *Geofluids*, **7**, 112.
47. A.Z. Al-Yaseri, M. Lebedev, A. Barifcani, S. Iglauer (2015). *Journal of Chemical Thermodynamics*, **93**, 416.
48. P. Chiquet, D. Broseta, S. Thibeau (2007). *Geofluids*, **7**, 112.
49. Y. Kim, J. Wan, T.J. Kneafsey, T.K. Tokunaga (2012). *Environmental Science & Technology*, **46**, 4228.
50. X. Zhang, J. Ge, F. Kamali, F. Othman, Y. Wang, F. Le-Hussain (2020). *Journal of Natural Gas Science and Engineering*, **73**, 103050.
51. Z. Dai, L. Xu, T. Xiao, B. McPherson, X. Zhang, L. Zheng, S. Dong, Z. Yang, M.R. Soltanian, C. Yang, et al. (2020). *Earth-Science Reviews*, **208**, 103265.
52. R. Juanes, E.J. Spiteri, F.M. Orr, M.J. Blunt (2006). *Water Resources Research*, **42**, 1.
53. S. Wang, K. Liu, J. Han, K. Ling, H. Wang, B. Jia (2019). *Applied Sciences*, **9**, 1686.
54. H.I. Petersen, W.F. Al-Masri, A. Rudra, S. Mohammadkhani, H. Sanei (2023). *Movable and non-movable hydrocarbon fractions in an oil-depleted sandstone reservoir considered for CO_2 storage, Nini West Field, Danish North Sea*. Int J Coal Geol, **280**, 104399.
55. S. Mohammadkhani, F. Al-Masri, W. Olsen (2023). *Results of CO_2 flooding experiments, Greensand Phase 2 WP3.1*, GEUS Report 2023/28.